

Dynamics of dissolved DNA polymers using a frequency-dependent dielectric constant

V. K. Saxena and L. L. Van Zandt

Department of Physics, Purdue University, West Lafayette, Indiana 47907

(Received 26 February 1990)

The dielectric response of DNA polymers dissolved in a water solution plays an important role in the determination of the effect of long-range nonbonded interactions on the vibrational dynamics of DNA. All existing calculations for DNA vibrational modes assume the water dielectric function to be constant, independent of the oscillation frequency. However, in real DNA solutions modes depend on the dielectric constant and the dielectric constant is strongly dependent on frequency, particularly in the frequency range $0-100\text{ cm}^{-1}$. We have extended our earlier effective-field approach for dissolved DNA polymers to include the important frequency dependence of the dielectric response function. Using the most recent experimental values for the system parameters, particularly dielectric relaxation time, we have calculated the phonon spectrum of the B-form poly(dA)-poly(dT) DNA polymer. [The notation poly(dA)-poly(dT) means that one strand contains adenine (A) bases, and the other only thiamine (T) bases.] Within a single model and with a single set of parameters our results agree with experimental data on speed of sound and inelastic neutron scattering. Besides this, our calculations also present some lines to be observed in poly(dA)-poly(dT) samples. We have analyzed the eigenvectors of all the modes in the range $0-120\text{ cm}^{-1}$ and have characterized them in terms of various types of motions such as propeller twist, base-roll, breathing mode, etc. As a result of the frequency-dependent behavior of the long-range forces some new and interesting features are predicted at low frequencies in the millimeter range.

I. INTRODUCTION

The importance of long-range interatomic interactions for the low-frequency spectrum of DNA has been well known since the calculations of low-frequency sound speed on a DNA polymer by Mei *et al.*¹ The Mei model of the long-range forces was developed in response to the appearance of experimental Brillouin scattering data by Maret *et al.*² Soon afterward, other confirming experimental data on a low-frequency spectrum of DNA were published. Hakim, Lindsay and Powell³ extended and confirmed the measurements of Maret *et al.* Recently, Grimm *et al.*⁴ have reported inelastic-neutron-scattering studies on ordered DNA material. In 1987, Powell *et al.*⁵ published infrared absorption spectra of oriented DNA films in the frequency range $50-110\text{ cm}^{-1}$ and reported four prominent resonances. Based on these experimental observations, during the past few years the importance of the long-range forces has been realized further and theoretical calculations have been performed to interpret the experimental data.⁶⁻⁹ Recently, we developed an effective-field approach for the treatment of long-range nonbonded interactions.^{10,11} Unlike earlier theoretical models (e.g., the Mei model of long-range forces), this model has been successful in explaining three different sets of experimental data; i.e., low-frequency sound speed, inelastic-neutron-scattering data, and mid-frequency resonances observed by Powell *et al.*, within a single set of parameters. All earlier interpretations of these data have required different parameter sets for each different experiment. The success of this model in ex-

plaining most of the existing experimental observations on DNA polymers shows it to be a very reliable theoretical model for DNA dynamics. The experimental observations and theoretical calculations during the past few years indicate that these nonbonded forces play an important role in the low-frequency and intermediate-frequency dynamics of DNA.

Even in earlier models it was recognized that the long-range interatomic interactions between distant atoms are not simple vacuum Coulombic interactions, but are modified by the presence of an intervening medium. In earlier models^{1,9,12,13} of long-range forces where these forces were accounted for by summing Coulomb-like forces over the atoms in 10-15 cells on each side of a central base pair, the effect of the intervening medium was incorporated in terms of an effective "dielectric constant," parametrized for each pair of interacting atoms according to their locations within the polymer chain. This approach is currently used by several authors.¹³⁻¹⁶ A very peculiar feature of one earlier model^{12,13} is the use of absolute values of partial charges on the polymer atoms; that is, all contributions to the force constants, once computed, are replaced by their absolute values. Without this curious and unphysical step, instabilities are often predicted by the calculation.

In our new model of long-range forces,^{10,11} we have avoided the use of large summations over various cells, the heuristic pairwise dielectric constants, and the artificial and unphysical use of absolute values of partial charges. Instead of individually summing over various cells, we explicitly introduce the local electric field acting

on the atomic partial charges. This field satisfies Maxwell's equations, which in turn give the global, long-range behavior of the fields and thus leads to the effective atomic interactions. The dynamic electromagnetic field accompanying the motion of partially charged atoms accounts for the effects of the intervening and surrounding media in a natural way. Because the fields extend out a considerable distance into the surrounding medium, application of local electromagnetic boundary conditions at the molecule-solvent interface incorporates the dielectric behavior of the medium, and the propagation characteristics of the fields through the molecule-solvent system account for the distance dependence of the atomic interactions. It is clear from these observations, however, that the electromagnetic behavior of the water-solvent surrounding medium contributes in an important way to the overall system dynamics.

In our first effective-field model,^{10,11} as well as in the earlier model, the dielectric constant of the intervening medium was taken to be a constant independent of frequency. This simplified the calculation of the vibrational modes of the DNA homopolymer to an $N \times N$ eigenvalue problem. (N is the total number of degrees of freedom of one monomer.) It was necessary, however, to use different values for the dielectric constants when explaining different experiments. Hence, the ϵ value used in Refs. 6 and 7 gave an enormous sound speed and the value used in Ref. 1 failed to describe the neutron-scattering curve. However, in reality the dielectric response of the surrounding aqueous medium is strongly frequency dependent. Particularly in the low- and intermediate-frequency ranges, the dielectric function of the medium varies sharply with frequency.¹⁷ Therefore, to get a more physical picture of the spectrum of dissolved DNA polymers in the millimeter-microwave range, this frequency dependence must properly be included.

In our first usage of this scheme, for certain nonbonded interactions of intermediate range, we also used some absolute-value signs as in the older Mei work. In the calculation presented here, we have completely eschewed this unnecessary and unphysical description. All charge-dependent interactions enter with their proper signs. The success of this calculation shows that the instabilities of the older approach are actually a consequence of the crudity of replacing a complete field description of the electromagnetic problem with a collection of arbitrary dielectric constants between atoms.

In this paper, we present a calculation of the vibrational spectrum of a dissolved DNA polymer, including the effect of a frequency-dependent dielectric function of the medium. In order to characterize the nature of various vibrational modes, we also have performed an analysis of the eigenvectors of all the low-frequency modes in the range 0–120 cm^{-1} in terms of various types of motions, such as propeller twist, base roll, hydrogen bond "breathing character," and base shift. Our calculations lead to new interpretations for some of the modes that had been interpreted earlier completely differently. A most interesting consequence of our calculations is the appearance of new features of the spectrum in the low-mid-

frequency range.

In Sec. II we discuss briefly the effective-field model and present the corresponding equations of motion for the DNA-water-counterion system, and also give the parameter values used in the calculations. The results of iterative calculations for the spectrum are presented in Sec. III, where we also present the results of the analysis of the eigenvectors in terms of various types of motions. We also discuss the possible interpretations of some of the observed modes in the far-infrared frequency range.

II. EFFECTIVE-FIELD MODEL

The equations of motion for the DNA-water sheath system can be written as¹⁰

$$-\omega^2 q_i^\alpha = \sum_{j,\beta} D_{ij}^{\alpha\beta} q_j^\beta + e_i' E_z - i\omega \Gamma_i (\bar{s} - q_i^\alpha \eta_i) \delta_{iP} \delta_{\alpha z} \quad (1)$$

and

$$-\omega^2 \bar{s} = -q^2 v_w^2 \bar{s} - \lambda' E_z - i\omega \sum_i \Gamma_i (q_i^z - \bar{s} / \eta_i) \delta_{iP} - i\gamma' \omega \bar{s}, \quad (2)$$

where ω is a frequency of the particular mode of DNA. $q_i^\alpha = \sqrt{m_i} \delta r_i^\alpha$ represents the mass-weighted displacement amplitude of atom i , of mass m_i , in the α ($=x, y, z$) direction with the corresponding coordinate r_i^α . $\bar{s} = \sqrt{a\rho s}$, where s represents the displacement amplitude of the near water sheath containing the counterions, ρ is the linear mass density of the sheath, and a is the helix rise. The first term on the right-hand side of Eq. (1) comprises, within the harmonic approximation, the bonded forces resulting from bond stretch, angle bend, and twist, and the Coulomb forces between partial charges within a unit cell. This also includes the van der Waals forces between pairs of atoms within the central cell and the nearest-neighbor cells. A collection of all these forces is contained in the force-constant matrix $D_{ij}^{\alpha\beta}$. The last term on the right-hand side of Eq. (1) is the damping force at the molecule-solvent interface, with a similar term in Eq. (2), the equation of motion for the water-counterion sheath. Equation (2) contains the term $-i\omega\gamma'\bar{s}$ for damping at the sheath-bulk water interface. $e_i' = e_i / \sqrt{m_i}$, where e_i is the partial charge on atom i . $\lambda' = \lambda / \sqrt{a\rho}$, with $-\lambda = -\sum_i e_i$ being the total charge of the counterions within the water sheath. We have assumed complete charge neutrality within the molecule-sheath system. The Poisson-Boltzmann theory indicates that this is correct to about 5%. The first term on the right-hand side of Eq. (2) represents the elastic contribution to the sheath motion, v_w being the sound speed in bulk water, and q the wave vector for propagation of the disturbance along the DNA-solvent system. $\eta_i \equiv \sqrt{a\rho/m_i}$. Kronecker deltas δ_{iP} and $\delta_{\alpha z}$ restrict the frictional coupling of the DNA to the water sheath via the coupling of the z component of the motion of phosphorus atoms on the two backbones to the longitudinal motion of the water. The damping parameter γ' is derived from bulk water.¹⁸

At the limit of infinite dilution, the local effective elec-

tric field E_z , acting on atomic partial charges, is given by¹⁰

$$E_z(\omega) = \frac{P_z(\omega)}{\epsilon_{in}} \left[\frac{i\sigma + \omega\epsilon_{out}}{\omega\epsilon_{in}} \frac{2}{\kappa r_1} \frac{H_1^1(\kappa r_1)}{H_0^1(\kappa r_1)} - 1 \right]^{-1}, \quad (3)$$

where r_1 is the radius of the cylinder defining the molecule-solvent interface. H_0^1 and H_1^1 are zeroth- and first-order Hankel functions of the first kind, and σ is the electrical conductivity of the solvent. ϵ_{in} is the average dielectric constant within the cylindrical region of the DNA and the water sheath. ϵ_{out} is the dielectric constant of the surrounding solvent medium. κ is a function of ω , σ , and the wave vector q given by

$$\kappa^2 = -(q^2 - \epsilon_{out}\mu_0\omega^2 - i\sigma\mu_0\omega), \quad (4)$$

where μ_0 is the well-known constant of magnetostatics. P_z is the local electric polarization density given by

$$P_z = \frac{1}{\pi r_1^2 a} \left[\sum_i e'_i q_i^z - \lambda' \bar{s} \right]. \quad (5)$$

In our earlier calculations^{10,11} we had assumed the dielectric constant ϵ_{out} of the surrounding medium to be a constant independent of frequency ω . Here we recognize that the frequency-dependent dielectric function of the medium $\epsilon_{out}(\omega)$ can be written as¹⁷

$$\epsilon_{out}(\omega) = \frac{\epsilon_{dc} - \epsilon_{\infty}}{1 + i\omega\tau_s} + \epsilon_{\infty}, \quad (6)$$

where ϵ_{dc} and ϵ_{∞} are the zero-frequency static dielectric constant and infinite-frequency dielectric constant of the aqueous medium, respectively. τ_s is the dielectric relaxation time of the solvent medium. The dielectric relaxation parameter τ_s of the solvent was taken to be 7.9×10^{-12} sec, the most recent value reported from microwave absorption measurements.¹⁹ This places the range of most rapid variation of ϵ_{out} around $50 \sim 100$ cm^{-1} .

As a result of the frequency dependence of the local-field terms and the damping terms, the set of equations (1) and (2) becomes nonlinear in ω^2 and cannot be solved by simple diagonalization. We have calculated the spectrum of B-form poly(dA)-poly(dT) DNA using this model. We used an iterative procedure to get the eigenmode frequencies and the corresponding eigenvectors for each of the modes separately. For the frequency-independent parts of the force-constant matrix $D_{ij}^{\alpha\beta}$, the damping coefficients, and the sound speed for bulk water, we used the same values as in our earlier calculations.^{10,11} As mentioned earlier, the Coulomb interactions within a base pair have been given their correct algebraic signs. Likewise, in the effective-field term the same earlier values of σ and r_1 were used. Brillouin scattering studies of DNA and its hydration shell²⁰ have shown that the dielectric relaxation time within the first hydration shell is 4.0×10^{-11} sec. In accord with this, in Eq. (3), we have taken a value of $2.0 \epsilon_0$ for ϵ_{in} , the dielectric constant of the cylindrical region containing the DNA helix and the primary hydration sheath. $\epsilon_0 = 8.854 \times 10^{-12}$ C²/n m² is

the permittivity of vacuum. In Eq. (6) for ϵ_{dc} , we have used a value of $68.0\epsilon_0$ corresponding to water with a counterion concentration²¹ of about 15%; for ϵ_{∞} we use a value $1.77\epsilon_0$.

III. RESULTS AND DISCUSSION

Using the model discussed in Sec. II, we performed an iterative calculation of the low- and intermediate-frequency vibrational modes of a poly(dA)-poly(dT) DNA homopolymer. In Fig. 1 we display the dispersion curves for modes ω as a function of the phase angle $\theta = q/a$. The low θ values of the frequencies for the compressional mode were used to calculate the low-frequency speed of sound for the polymer, which turned out to be 1890 m/sec. The experimental value³ is 1800 m/sec. The procedure described in Ref. 6 was used to calculate the inelastic-neutron-scattering curve. These results, along with the experimental points of Grimm *et al.*,⁴ are also displayed in Fig. 1. It can be seen that the theoretical curve is in reasonable agreement with the experimental observations. The experimental data were obtained for precipitated wet-spun DNA fibers equilibrated to 75% relative humidity. The theory, of course, is for infinitely dilute solutions. Therefore, clearly, the experimental samples do not necessarily correspond exactly to the hy-

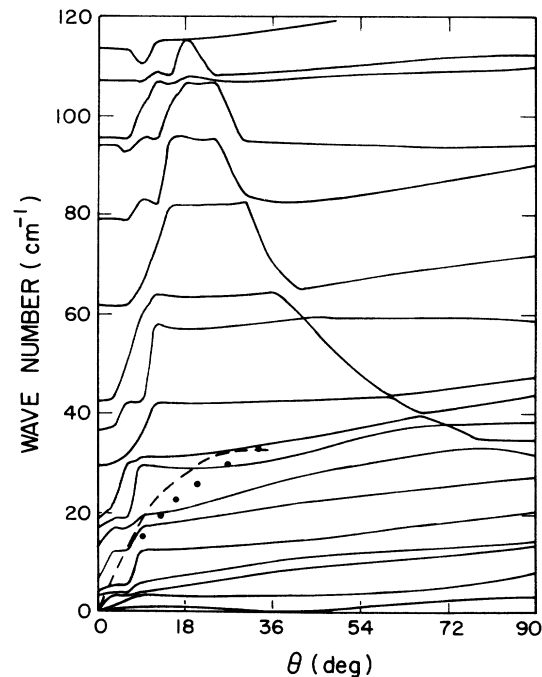


FIG. 1. Dispersion curves for the modes below 120 cm^{-1} for a poly(dA)-poly(dT) homopolymer. The dashed curve is the mapping of the compressional mode for comparison with the neutron scattering points shown by solid circles.

dration used in the present theory. We plan to repeat calculations for the case of dry material, similar to the Dorfman–Van Zandt¹⁸ model of low-water material to verify that there is no essential difference between the two cases as far as the neutron-scattering data are concerned.

The interpretation and characterization of some modes observed in the far-infrared frequency range⁵ have been a controversial issue during the last two years. Particularly, a mode observed at 63 cm^{-1} in vacuum-dried, free-standing, unoriented films of polycrystalline poly(dA)-poly(dT) has been interpreted in various ways. Young, Prabhu, and Prohofsky⁹ have suggested that this mode arises as a result of a propeller-twisted conformation in a B-form A-T polynucleotide. These same authors also, have more or less simultaneously offered other possible interpretations to characterize this mode.⁸ In our present model we predict a mode at around this frequency: precisely at 61.63 cm^{-1} for $\theta=0^\circ$ corresponding to the longitudinal excitations, and at 64.36 cm^{-1} for $\theta=36^\circ$ (transverse polarized excitation). In order to characterize the nature of motion involved with this and other modes in the low- and intermediate-frequency range, we performed an analysis of the eigenvectors of these modes in terms of various types of motions. The *propeller twist* of a base pair is defined as the relative angular displacement between the average planes of the two bases rotated in opposite directions about a long axis, determined by the two nitrogen—carbon bonds joining each base with its associated sugar. Similarly, a *base roll* describes the motion in which both bases, taken as a rigid unit, rotate about the same long axis through the two base-sugar links. In order to analyze the motions, we constructed standard vectors representing these types of motions. The projections of an eigenvector along these standard vectors then determined the fractional amount of each motional type possessed by that mode. We also analyzed the eigenvectors for possible “breathing” character, which is defined as relative displacement in opposite directions of the two bases along the same long axis defined above. Finally, we examined another possible motion, which we call base shift, where the two bases, as a rigid unit, displace together along the long axis. We performed this analysis both for longitudinal as well as transverse excitations, that is, at $\theta=0^\circ$ and 36° . The results are tabulated in Tables I and II for all the modes below 120 cm^{-1} . In these tables R_- , R_+ , T_- , and T_+ represent the fractional motion of various modes corresponding to the propeller twist, base roll, breathing mode, and base shift, respectively.

Contrary to the claim made by Young, Prabhu, and Prohofsky,⁹ we find that the mode around 63 cm^{-1} does not have the character of a propeller-twist-type motion. This illustrates that the overall dynamical behavior of the system in this frequency range is rather sensitive to the details of the model used for the calculations of vibrational dynamics. Both for longitudinal as well as transverse polarizations we find this mode has a strong breathing-mode character. Modes around 95, 107, and 170 cm^{-1} are found to have weaker breathing character. The strongest propeller-twist character is found for the mode near 42 cm^{-1} . The other modes that show a weaker propeller-twist character lie near the frequencies 36, 96,

TABLE I. Values of fractional propeller-twist (R_-), base-roll (R_+), hydrogen-bond breathing (T_-), and base-shift (T_+) motions for the modes below 120 cm^{-1} of a poly(dA)-poly(dT) homopolymer at the zone center $\theta=0^\circ$. ω is in cm^{-1} .

ω	R_-	R_+	T_-	T_+
2.97	0.004 074	0.000 002	0.002 390	0.002 287
3.67	0.004 602	0.000 007	0.004 007	0.003 361
5.73	0.015 426	0.005 776	0.000 001	0.079 672
12.72	0.000 295	0.008 289	0.000 123	0.182 135
16.76	0.004 012	0.000 031	0.015 290	0.027 290
18.70	0.001 331	0.000 604	0.067 014	0.002 655
29.69	0.098 612	0.010 009	0.002 337	0.003 952
36.64	0.197 715	0.154 554	0.016 899	0.000 689
42.65	0.599 493	0.073 342	0.008 350	0.000 404
61.63	0.076 076	0.002 055	0.650 084	0.005 965
79.01	0.007 426	0.052 602	0.037 702	0.004 570
93.96	0.003 613	0.023 825	0.014 797	0.014 598
95.59	0.175 758	0.000 020	0.107 276	0.000 020
106.97	0.045 714	0.001 126	0.261 782	0.011 369
113.40	0.011 134	0.000 315	0.019 460	0.002 633
114.79	0.010 141	0.000 305	0.010 285	0.007 490

and 139 cm^{-1} . At $\theta=0^\circ$ the strongest base-roll character is found in the mode around 37 cm^{-1} , whereas for $\theta=36^\circ$ the mode near 64 cm^{-1} possesses the strongest base roll. For longitudinal polarization the mode around 12 cm^{-1} has the strongest base shift but for transverse polarization the lowest mode, which is also a bending mode, at zero frequency has the strongest base shift. It would seem that explicit *eigenvector* information would be very useful for sorting out the correspondence between theory and experiment. Frequency measurements alone are ambiguous.²²

TABLE II. Values of fractional propeller-twist (R_-), base-roll (R_+), hydrogen-bond breathing (T_-), and base-shift (T_+) motions for the modes below 120 cm^{-1} of a poly(dA)-poly(dT) homopolymer at $\theta=36^\circ$. ω is in cm^{-1} .

ω	R_-	R_+	T_-	T_+
0.00	0.000 000	0.000 000	0.000 127	0.105 129
2.92	0.002 438	0.007 525	0.000 437	0.350 045
7.72	0.001 046	0.000 849	0.032 542	0.028 055
10.01	0.008 697	0.001 564	0.001 642	0.020 879
13.92	0.000 967	0.013 033	0.000 136	0.070 431
21.27	0.003 188	0.007 849	0.003 095	0.018 545
26.13	0.020 319	0.013 732	0.060 880	0.013 002
30.67	0.072 600	0.008 403	0.016 260	0.004 484
33.93	0.063 687	0.052 500	0.003 195	0.007 504
42.29	0.736 267	0.015 510	0.017 120	0.001 248
58.33	0.060 735	0.091 391	0.027 277	0.000 335
64.36	0.045 456	0.111 836	0.537 071	0.009 308
69.29	0.002 609	0.000 143	0.000 050	0.000 124
82.44	0.010 197	0.004 746	0.031 902	0.000 323
94.64	0.176 433	0.004 503	0.125 215	0.000 859
107.14	0.031 715	0.000 515	0.153 248	0.028 727
108.50	0.040 531	0.000 965	0.126 490	0.007 213
117.12	0.011 577	0.001 033	0.009 796	0.001 852

Finally, in Table III we have given the transition dipole moments associated with each mode [specifically, p_z for the modes at $\theta=0^\circ$ and $p_\perp=(p_x^2+p_y^2)^{1/2}$ for those at $\theta=36^\circ$]. We should point out that our dipole moments are quite weak for the modes near 63 cm^{-1} , although the experimental absorptions are strong.

We ran our iterative calculation for very small angles ($\theta \leq 1^\circ$) for the low-frequency modes and found some totally new and peculiar features. At very small angles, for $\theta \approx 0^\circ$, the compressional mode, as is expected and is well known, is linear in θ ; then it shows a dip (negative slope), for a very small range of θ , reaching a minimum, and finally rising almost linearly with θ . We have not displayed these features in Fig. 1. The low-frequency sound speed can be extracted from the linear region of this curve near $\theta \approx 0^\circ$. However, the existence of a change of curvature and a minimum is a completely new feature. One must attribute this predicted behavior to the variation of the dielectric constant of the medium in the very-low-frequency region. In fact, some very interesting behavior is going on in the GHz-frequency range. Unfortunately, the spectroscopic methods so far used for DNA in solution have not been able to give a clear picture of the spectrum of DNA in the low- and intermediate-frequency range because of strong water absorption. Finally, it is worth comparing our present results with those of our earlier calculations using a constant frequency-independent dielectric constant.¹¹ At $\theta=0^\circ$ some of the modes in the present calculation are shifted. The mode, which in our earlier calculation was found to be at 21.15 cm^{-1} , is shifted down to 18.92 cm^{-1} . The mode at 61.63 cm^{-1} has been shifted down from 67.31 cm^{-1} and comes nearer to the experimentally observed mode⁵ around 63 cm^{-1} . More small changes are observed for $\theta=36^\circ$. One of the most important and interesting features found in the present calculation is the behavior of the compressional mode. This mode is found

TABLE III. Values of the transition dipole moments p_z (at $\theta=0^\circ$) and p_\perp (at $\theta=36^\circ$).

$\theta=0^\circ$		$\theta=36^\circ$	
$\omega\text{ (cm}^{-1}\text{)}$	p_z	$\omega\text{ (cm}^{-1}\text{)}$	p_\perp
0.00	0.000 000	0.00	0.006 035
0.00	0.002 949	2.92	0.003 141
0.00	0.003 140	7.72	0.000 067
2.97	0.000 288	10.01	0.000 154
3.67	0.000 062	13.92	0.000 455
5.73	0.002 209	21.27	0.000 252
12.72	0.000 938	26.13	0.005 317
16.76	0.000 012	30.67	0.001 360
18.70	0.000 037	33.93	0.001 338
29.69	0.000 001	42.29	0.001 523
36.64	0.003 005	58.33	0.001 260
42.65	0.000 552	64.36	0.001 023
61.63	0.000 278	69.29	0.000 739
79.01	0.002 175	82.44	0.003 300
93.96	0.009 621	94.64	0.000 678
95.59	0.001 250	107.14	0.006 146
106.97	0.000 205	108.50	0.004 449
113.40	0.004 759	117.12	0.001 066
114.79	0.001 708	127.27	0.000 086

to follow the experimentally observed curve, from inelastic neutron scattering. The progress of the compressional character up through a series of band crossings is most sharply delineated in the present calculation, compared to the earlier efforts.^{6,7}

ACKNOWLEDGMENTS

This work was performed under Office of Naval Research Contract No. N00014-87-K-0162 funded by the Strategic Defense Initiative Organization.

¹W. N. Mei, M. Kohli, E. W. Prohofsky, and L. L. Van Zandt, *Biopolymers* **20**, 833 (1981).

²G. Maret, R. Oldenbourg, D. Dransfeld, and A. Rupprecht, *Colloid Polym. Sci.* **257**, 1017 (1979).

³M. B. Hakim, S. M. Lindsay, and J. Powell, *Biopolymers* **23**, 1185 (1984).

⁴H. Grimm, H. Stiller, C. F. Majkrzak, and A. Rupprecht, *Phys. Rev. Lett.* **59**, 1780 (1987).

⁵J. W. Powell *et al.*, *Phys. Rev. A* **35**, 3929 (1987).

⁶W. K. Schroll, V. V. Prabhu, E. W. Prohofsky, and L. L. Van Zandt, *Biopolymers* **28**, 1189 (1988).

⁷V. V. Prabhu, W. K. Schroll, L. L. Van Zandt, and E. W. Prohofsky, *Phys. Rev. Lett.* **60**, 1587 (1988).

⁸K. M. Awati and E. W. Prohofsky, *Phys. Rev. A* **40**, 497 (1989).

⁹L. Young, V. V. Prabhu, and E. W. Prohofsky, *Phys. Rev. A* **40**, 5451 (1989).

¹⁰V. K. Saxena, L. L. Van Zandt, and W. K. Schroll, *Phys. Rev. A* **39**, 1474 (1989).

¹¹L. L. Van Zandt and V. K. Saxena, *Phys. Rev. A* **39**, 2672 (1989).

¹²K. V. Devi-Prasad and E. W. Prohofsky, *Biopolymers* **23**, 1795 (1984).

¹³V. V. Prabhu, L. Young, and E. W. Prohofsky, *Phys. Rev. B* **39**, 5436 (1989).

¹⁴P. A. Kollman, P. K. Weiner, G. Quigley, and A. Wang, *Biopolymers* **21**, 1945 (1982).

¹⁵B. Tidor, K. K. Ikikura, B. R. Brooks, and M. Karplus, *J. Biomol. Struct. Dyn.* **1**, 231 (1983).

¹⁶K. K. Ikikura, B. Tidor, B. R. Brooks, and M. Karplus, *Science* **229**, 571 (1985).

¹⁷R. Pethig, *Dielectric and Electronic Properties of Biological Materials* (Wiley, New York, 1979).

¹⁸B. H. Dorfman and L. L. Van Zandt, *Biopolymers* **23**, 913 (1984).

¹⁹H. R. Garner, A. C. Lewis, and T. Ohkawa (unpublished).

²⁰N. J. Tao, S. M. Lindsay, and A. Rupprecht, *Biopolymers* **27**, 1655 (1988).

²¹J. B. Hubbard, L. Onsager, W. M. Van Beek, and M. Mandel, *Proc. Natl. Acad. Sci. (U.S.A.)* **74**, 401 (1977).

²²L. L. Van Zandt and V. K. Saxena, *Biopolymers* **30**, 87 (1990).